

STUDY ON VERTICAL ELECTROPOLISHING OF NINE-CELL NIOBIUM COUPON CAVITY

V. Chouhan[†], Y. Ida, K. Nii, T. Yamaguchi, Marui Galvanizing Co., Ltd, Himeji, Japan
H. Hayano, S. Kato, H. Monjushiro, T. Saeki, M. Sawabe, High Energy Accelerator Research Organization (KEK), Tsukuba, Japan

Abstract

We report a study on vertical electropolishing (VEP) performed for a 1.3-GHz nine-cell niobium (Nb) coupon cavity using a unique cathode called Ninja Cathode. The design of the cathode for VEP of a nine-cell cavity was based on the Ninja cathode used for single-cell cavity since the Ninja cathode reduced longitudinal asymmetry in material removal and yielded smooth surface of the single-cell cavity. Moreover, single-cell Nb cavities after being treated in VEP using Ninja cathodes showed good performance in vertical RF tests. The nine-cell coupon cavity used in this study was designed to have totally nine coupons set on the iris and equator positions of the first, fifth and ninth cells. These three cells also contain viewports near the upper and lower iris positions. Measurement of currents for the individual coupons and in-situ observation are possible using the viewports to understand EP phenomenon at different locations of the cavity. VEP results, which include removal thicknesses at different positions of the cavity and surface study of the coupons, are discussed.

INTRODUCTION

Electropolishing (EP) process is adopted as the final surface treatment of niobium (Nb) superconducting RF cavities to achieve their good performance in terms of field gradient and quality factor. A cavity is currently electropolished (EPed) in a horizontal posture in the so-called horizontal EP process. A vertical EP (VEP) process, which supposed to be a cost effective method, is currently under research for optimization of EP parameters. Earlier we have introduced the issues, which appear in the VEP process, including longitudinal asymmetric removal and rough surface of a cavity [1]. In order to minimize the issues, a unique cathode called Ninja cathode with four retractable blades was developed and applied to single-cell cavities. The cathode minimized removal asymmetry and roughness of the entire surface inside the cavities [2–4].

This work describes application of the Ninja cathode on the nine-cell coupon cavity [5, 6] and its effect on the cavity surface and removal.

EXPERIMENT

Ninja Cathode

The Ninja cathode for a nine-cell cavity was prepared

[†] vchouhan@e-marui.jp

with the similar design that of the Ninja cathode applied to the single-cell cavity as reported elsewhere [4]. The Ninja cathode for a nine-cell cavity contained 3 insulating blades and covered with PTFE meshed sheet to reduce a number density of H₂ bubbles in the cavity cells.

Nine-cell Coupon Cavity

A nine-cell coupon cavity (9-CCC) was designed to have nine coupons set at different locations of the cavity. The first (top), fifth (center) and ninth (bottom) cells contain coupons at the equator and near upper, and lower iris positions. The coupons at the irises were set with viewports. Figure 1 shows schematic of cavity with positions of the coupons and viewports. The detail of the 9-CCC is given in Ref. [5]. EP currents from the individual coupons and cavity can be measured. The viewports were used to take movies and observe behaviour of gas bubbles and the effect of blades on the cavity surface.

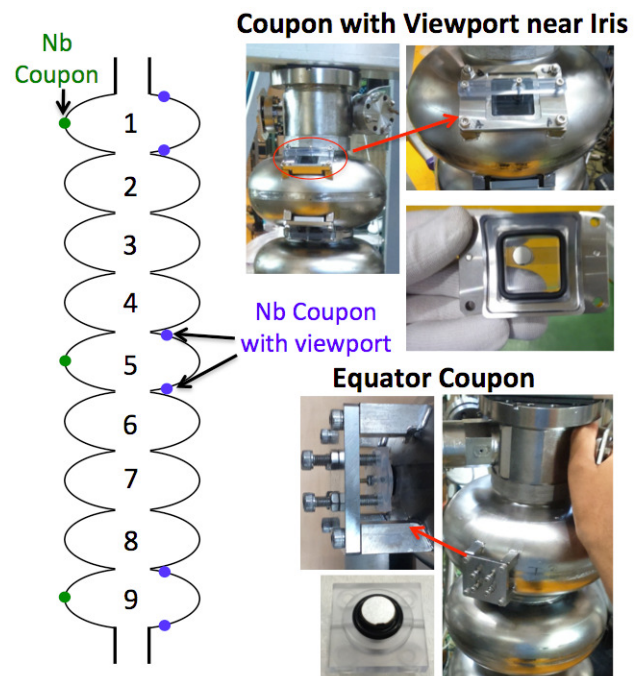


Figure 1: Photographs and schematic show coupons and viewports and their positions at irises and equator.

VEP Setup

A system was designed to perform VEP of nine-cell and single-cell cavities. The system is equipped with separate acid and water pipelines, flow meters, an acid reservoir, water spray facility for cooling of the cavity, a water reservoir for spray water, heat exchangers for the

acid and water reservoir, and chillers. The system is controlled by a touch panel screen. Figure 2 shows the 9-CCC set on the VEP stand. A power supply with a maximum voltage of 20 V and current of 300 A was used. Thermocouples were set at the top iris, bottom iris and equator positions of the top, center and bottom cells. Voltage, temperatures, and coupon and cavity currents were logged.



Figure 2: 9-CCC at the VEP stand.

Two VEP experiments were performed with the same Ninja cathode whereas cavity temperature and cathode rotation speeds were different in both the VEP experiments.

RESULTS

Polarization Curves for Coupons

Polarization curves (I-V curves) for the coupons provide information of electro-chemical phenomenon occurring on the cavity surface as a function of applied voltage [2, 3]. I-V tests were performed at several rotation speeds of the cathode before performing a long-time VEP of the cavity. These tests were aimed to find EP plateaus in I-V curves. Coupon current densities as a function of voltage at cathode rotation speeds of 0, 20 and 50 rpm are shown in Fig. 3 and 4. The I-V curves in Fig. 3 were obtained at a cavity temperature of $\sim 25^\circ\text{C}$ while the I-V curves in Fig. 4 were obtained at a lower cavity temperature of less than 15°C . At the high temperature and 0 rpm, EP plateaus were not seen in the I-V curves of the top iris coupon in the top cell and the equator coupons in the top and center cell. The curves were shifted to the higher voltage side at higher rotation speeds. Similar effect of rotation speed was observed in VEP of the single-cell coupon cavity [2, 3]. EP plateaus were apparent for all the nine coupons at the low temperature even though the cathode rotation speed was 50 rpm.

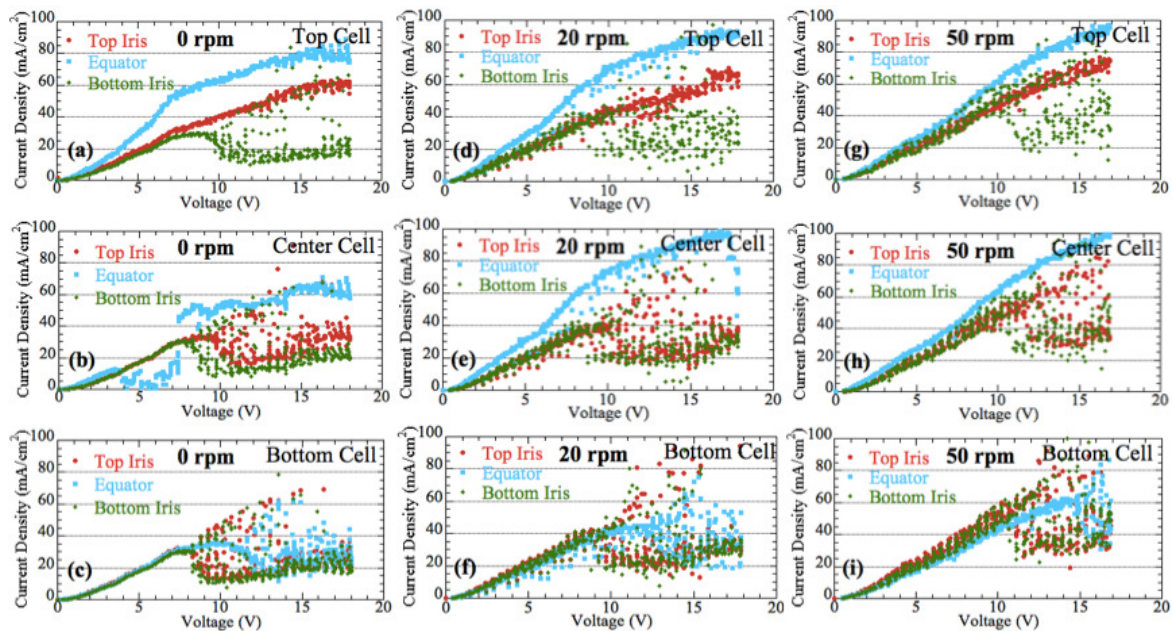


Figure 3: Polarization curves for the coupons located in the top, center, and bottom cells at the high temperature ($\sim 25^\circ\text{C}$) and cathode rotation speeds of (a-c) 0 rpm, (d-f) 20 rpm and (g-i) 50 rpm.

Content from this work may be used under the terms of the CC BY 3.0 licence (© 2017). Any distribution of this work must maintain attribution to the author(s), title of the work, publisher, and DOI.

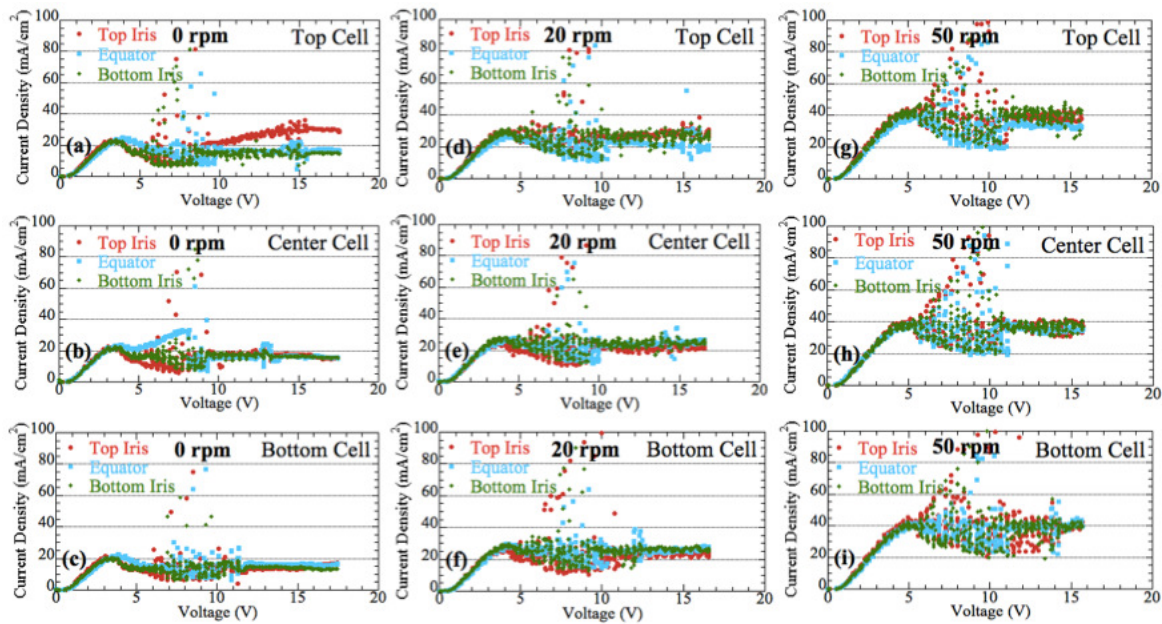


Figure 4: Polarization curves for the coupons located in the top, center, and bottom cells at the low temperature ($<15^{\circ}\text{C}$) and cathode rotation speeds of (a-c) 0 rpm, (d-f) 20 rpm and (g-i) 50 rpm.

VEP of Cavity

VEP-1 was performed at the high temperature and a cathode rotation speed of 50 rpm [6]. During the VEP process cavity temperature increased over 30°C since the chiller capacity was not enough to control the cavity temperature. In the case of VEP-2, two parameters were modified. (1) Cavity temperature was controlled below 17°C using a high capacity chiller for acid cooling and (2) a rotation speed of the cathode was set at 20 rpm. The rotation speed of 20 rpm was selected because it was found adequate to obtain symmetric removal and smooth surface of the single-cell coupon cavity. A voltage of $\sim 12\text{ V}$ and an acid flow rate of $\sim 5\text{ L/min}$ were applied in both the VEP processes. The current and temperature profiles in both the VEP processes are shown in Fig. 5. Average cavity removal thicknesses calculated by integrated electric charge were 23 and $37\ \mu\text{m}$ in VEP-1 and 2, respectively.

Observation through Viewports

Bubble behaviour at the top iris positions was observed through the viewports. The photographs of the viewports near the top iris positions in VEP-2 are shown in Fig. 6. A huge amount of bubbles was found in the top cell and bubbles homogeneously covered the top iris surface. The bubble quantity in the center cell was comparatively less while the bubbles stayed on the viewport surface for a longer time with slow movement in upward direction. In the bottom cell, bubbles quantity was found to be further less while bubble movement on the viewport was faster than that observed in the center cell. The effect of cathode rotation was found not significant to displace bubbles from the surface. The behaviour of bubbles was quite similar in VEP-1 also, while the quantity of bubbles in the top cell seemed to be larger than that in VEP-2.

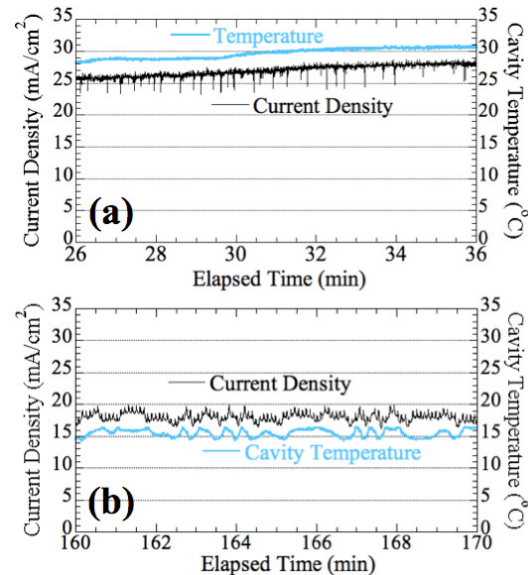


Figure 5: Cavity current density and temperature profiles in (a) VEP-1, and (b) VEP-2.

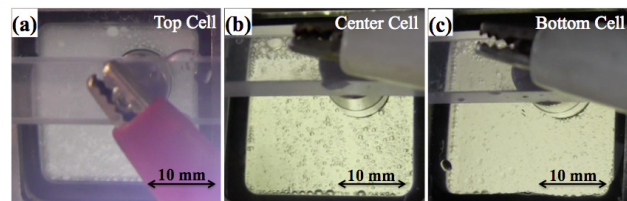


Figure 6: Top iris viewports at (a) top, (b) center, and (c) bottom cells.

Surface Features of Coupons

The coupon surfaces after both the VEP experiments were observed with optical microscope and their surface

roughness was measured using a surface profiler. The images of the coupons after VEP-1 and 2 are shown in Figs. 7 and 8, respectively. Surface roughness (R_z) of the coupons is compared in Fig. 9. The coupons were very rough after VEP-1, whereas the VEP-2 yielded shiny surfaces of the coupons as observed visually. The optical microscope images and roughness data clearly show the differences in the coupon surfaces after VEP-1 and 2. After VEP-1, rough equator surfaces in all the cells and the top iris surface in the top cell were microscopically rough with roughness R_z of 9–14 μm and result of etching of Nb instead of polishing. Other coupon surfaces after VEP-1 were also rough with roughness R_z of ~ 4 to 5 μm . After VEP-2, roughness of all the coupons except the top iris in the center cell was between 1 to 1.8 μm . The top iris coupon in the center cell suffered with bubble traces and was macroscopically rough with roughness R_z measured to be ~ 5 μm . The top iris surface in the top cell was also influenced by the large amount of bubbles. However, the surface was not rough.

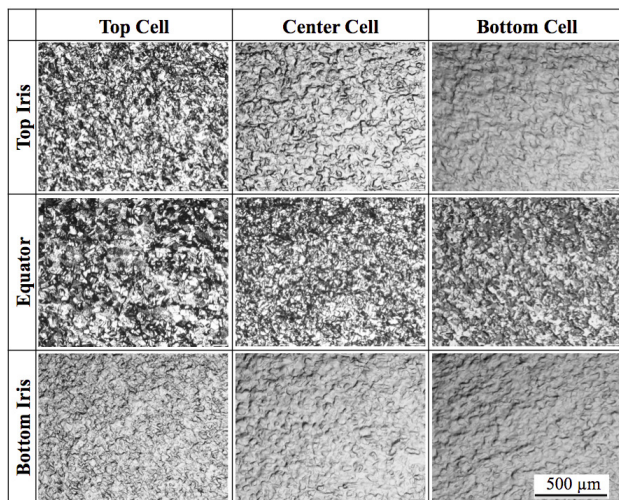


Figure 7: Optical microscope images of the coupons after VEP-1.

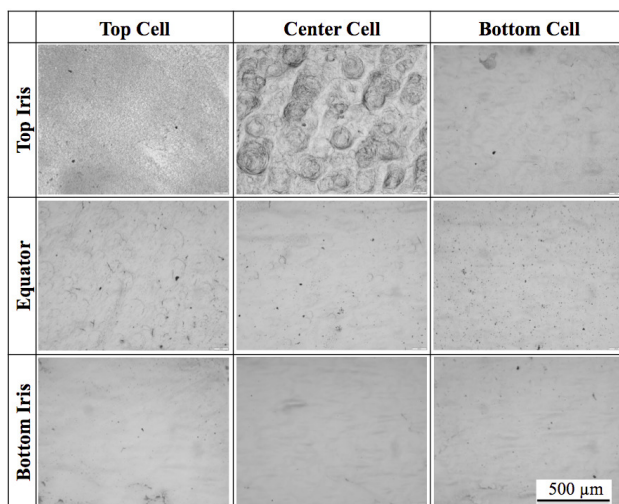


Figure 8: Optical microscope images of the coupons after VEP-2.

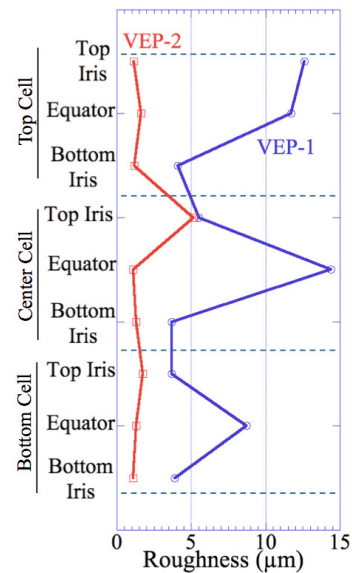


Figure 9: Roughness (R_z) of the coupon surfaces after VEP-1 and 2.

Removal Trends

Cavity wall thicknesses at many positions as show in the Fig. 10 were measured before and after both the VEP processes to calculate removal along the cavity length. The removal thicknesses were plotted as a function of the cavity length as shown in Fig. 10. Removal in VEP-1 seems to be less asymmetric than in VEP-2. In VEP-2 each cell represents higher removal at the top iris compared to that at the equator and bottom iris. Removal at the top irises was increasing towards the upper cells and hence larger removal asymmetry in the upper cells. The removal thicknesses at the bottom iris and equator positions were found to be similar in all the cells.

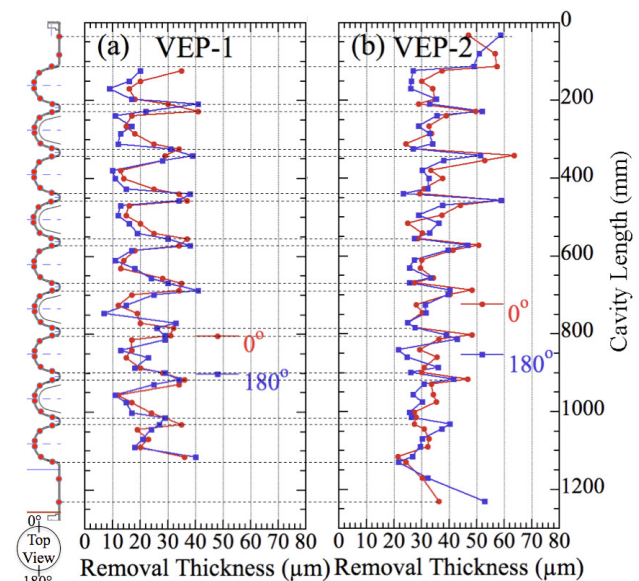


Figure 10: Trends of removal thicknesses along the cavity length in (a) VEP-1, and (b) VEP-2. The points on cavity schematic show positions of thickness measurement.

DISCUSSION

The high temperature enhanced the total EP current and hence higher amount of H₂ bubbles generated at the cathode surface. The higher amount of bubbles enhanced the screening of the cathode surface to reduce an electric field on the Nb surface. Other than this, a high temperature can reduce dynamic viscosity of electrolyte and enhance diffusion coefficient which might dominate over development of dielectric layer of Nb₂O₅ [7, 8]. These effects of high temperature prevent obtaining an optimum EP condition. The effect of high temperature was reflected in the polarization curves of coupons. Since the adverse effects of high temperature might be reduced by lowering the temperature from ~30 to 15°C, EP plateaus appeared clearly in the polarization curves of the coupons.

EP performed at the voltage lying in the plateau regions resulted in the smooth surface of the coupons. The bubbles on the surface in the center cell were staying for a longer time and might enhanced the EP rate locally to yield a macroscopic rough surface. The grain boundaries were not etched because removal occurred under the mass-controlled condition. Since the bubbles covered the top iris surface in the top cell homogeneously and were replaced by other bubbles quickly, bubble footprints and rough surface were not found for the top iris coupon in the top cell. The less number of bubbles and shorter residence time of bubbles on the top iris surface in the bottom cell resulted in the smooth surface of the top iris coupon. Similar behaviour of the bubbles and impact of their residence time on the Nb surface was noticed in the single cell cavity [1–3].

The higher amount of bubbles accumulated on the top iris surfaces in the upper cells, as observed from the viewports, might enhance the removal in the upper cells [1–3]. The lower rotation speed of the cathode in VEP-2 might be the cause of larger asymmetry in removal. Our previous study on laboratory EP of small samples and VEP of the single-cell coupon cavity showed the impact of bubbles on removal, and effect of cathode rotation speeds [2, 3].

CONCLUSION

Two VEP experiments were performed with the nine-cell coupon cavity and the Ninja cathode at different cavity temperatures and cathode rotation speeds. The effect of temperature was clearly observed in I-V curves obtained for the nine coupons which were set at the iris and equator positions of the top, center, and bottom cells. In VEP-1 performed at a higher temperature, polishing plateaus were not seen for the equator coupons in the center, and top cells and the top iris coupon in the top cell. In VEP-2,

the I-V curves obtained at the low temperature were found with apparent EP plateaus for all the coupons. The VEP-1, performed at the high temperature reached over 30°C and with the Ninja cathode rotating at 50 rpm, resulted in rough surfaces of the coupons with Rz ranging from 4 to 14 μm. Since the VEP-2 was performed at the low temperature of ~15°C, lower cathode rotation speed of 20 rpm, and adequate voltage lying in the polishing region, this VEP resulted in smooth surfaces of the coupons. The effect of bubbles was noticed on the top iris coupon surface in the center cell. However, the surface smoothness was greatly improved in VEP-2. Longitudinal asymmetry was noticed in VEP-2 might relate to the accumulation of bubbles in the upper cells.

In order to solve the existing issues related to bubbles, the shape of the cathode blades, the cathode rotation speed, and acid flow rate will be optimized. The optimized parameters will be applied to a nine-cell cavity to evaluate RF performance of the cavity.

REFERENCES

- [1] V. Chouhan *et al.*, “Vertical Electropolishing of Nb Coupon Cavity and Surface Study of the Coupon Samples”, in *Proc. 27th Linear Accelerator Conf. (LINAC'14)*, Geneva, Switzerland, September 2014, paper THPP098, pp. 1080–1083.
- [2] V. Chouhan *et al.*, “Symmetric Removal of Niobium Superconducting RF Cavity in Vertical Electropolishing”, in *Proc. 17th Int. Conf. on RF Superconductivity (SRF'15)*, Whistler, Canada, September 2015, paper MOPB105, pp. 409–413.
- [3] V. Chouhan *et al.*, “Recent Development in Vertical Electropolishing”, in *Proc. 17th Int. Conf. on RF Superconductivity (SRF'15)*, Whistler, Canada, September 2015, paper THBA02, pp. 1024–1030.
- [4] V. Chouhan *et al.*, “Study of the Surface and Performance of Single-Cell Nb Cavities after Vertical EP Using Ninja Cathodes”, in *Proc. 28th Linear Accelerator Conf. (LINAC'16)*, East Lansing, USA, September 2016, paper MOPLR038, pp. 217–219.
- [5] S. Kato *et al.*, “Fabrication of nine-Cell Coupon Cavity for Vertical Electropolishing Test”, in *Proc. 28th Linear Accelerator Conf. (LINAC'16)*, East Lansing, USA, September 2016, paper MOPLR038, pp. 220–222.
- [6] K. Nii *et al.*, “Development of new type “Ninja” cathode for Nb 9-cell cavity and experiment of vertical electropolishing”, in *Proc. 28th Linear Accelerator Conf. (LINAC'16)*, East Lansing, USA, September 2016, paper MOPLR039, pp. 223–225.
- [7] H. Tian, and C. E. Reece, “Evaluation of the diffusion coefficient of fluorine during the electropolishing of niobium”, *Phys. Rev. ST Accel. Beams*, vol. 13, p. 083502, 2010.
- [8] A. C. Crawford, “Extreme diffusion limited electropolishing of niobium radiofrequency cavities”, *Nucl. Instr. Meth.*, vol. 849, pp. 5–10, 2017.